Effects of Density and Distribution of Non-Spontaneous Myocytes, Scars and Fibroblasts Inside the Human Sinoatrial Node

Eugenio Ricci[1], Chiara Bartolucci[1], Stefano Severi[1]

[1]University of Bologna, Cesena, Italy

Abstract

This work aims to elucidate the effects of structural and functional heterogeneity within the sinoatrial node tissue on its synchronization process. This is obtained by positioning either randomly or in clusters different densities of three types of cells: non-spontaneous myocytes, scars or fibroblasts. For each condition, four levels of heterogeneity (σ) in cellular electrophysiological properties are examined. The results show that the presence of non-spontaneous cells does not avoid frequency entrainment. The cycle length (CL) of the tissue shortens with higher σ and with cluster distribution. Opposite to this, randomly distributed scars prevent the tissue from synchronizing in frequency (standard deviation of CL increases with σ and density). Moderate presence of fibroblasts (up to 40%) supply physiologic rates ($CL \sim 800\,\mathrm{ms}$), whereas higher rates ($CL < 500\,\mathrm{ms}$) are obtained at upregulated levels (60%) of fibrosis with cluster distribution. Specific configurations lead to complex behaviours with high frequency ($CL_{mean} = 438\,\mathrm{ms}$) and spiral wave-like patterns. In conclusion, high density of randomly-distributed scar tissue and of cluster-distributed fibroblasts appear as unrealistic or pathological conditions.

1. Introduction

The sinoatrial node (SAN) is known to be the physiological source of the heart beat. This fundamental role is achieved thanks to many electrophysiological, geometrical and mechanical characteristics. Thus, the properties of the cells composing the SAN and their distribution inside this complex structure are of uttermost importance in determining its function. Recent works have highlighted the surprising heterogeneity of cells inside the SAN: e.g. more than 40% of the tissue was found to be fibrotic in healthy, adult human males [1], a value much higher than in the near atrium. This relevant amount of fibrosis inside the SAN could represent a protection mechanism: in order to avoid excessive hyperpolarization and stretch coming from the atrium, fibrosis provides electrical and mechanical shielding. This fact is supported by evidences of a continuous border (except for specific exit pathways) of fibrosis and fat around the SAN [2] and by the fact that fibrotic content increases with age and animal species size, quantities positively correlated with heart dimensions (and thus to electrical and mechanical strain). Additionally, it has been proven that fibroblasts can establish connections with myocytes inside the SAN [3] and that they express specific ionic channels allowing them to respond to stretch. Thus, being an electrically and mechanically active cell phenotype, they directly participate to the rhythmic activity of the SAN, as shown by computational studies on rabbit SAN models [4]. Fibrosis is also known to have a role in pathogenesis, and has been implicated in sinus node dysfunction (SND). Limiting the interconnections between myocytes indeed, fibrosis could prevent them from reaching an entrained condition, possibly leading to arrhythmias. The mechanism is however still not understood, since a correlation between the amount of fibrotic tissue and SND has not been demonstrated yet [2].

This work aims to evaluate the effects of different levels of fibrosis inside the SAN through a human SAN computational model. To do this, three different conditions - the presence of non-spontaneous cells, unexcitable myocytes (mimicking a scar) and fibroblasts - were tested inside a 2D SAN tissue at different densities (D, range 0-60%) and cellular heterogeneities ($\sigma = 0.1, 0.2, 0.3, 0.4$). Besides the density, the effects of the distribution were also assessed by positioning the cell types randomly or in clusters. The Cycle Length (CL) and the number of beating cells were computed in order to estimate the effects in terms of rate and entrainment between cells.

2. Methods

2.1. Cellular Coupling and Heterogeneity

A 2D discrete model was developed using the single cell human SAN model by Fabbri et al. [5]. To account

 ISSN: 2325-887X DOI: 10.22489/CinC.2021.208

for the electrical interaction between cells, the membrane voltage (V_m) update equation was modified by adding the gap junction current term (modeled through Ohm's law):

$$\frac{dV_m}{dt} = \frac{-i_{tot}}{C_m} + \frac{V_{net}}{R_{gap} \cdot C_m},$$

where i_{tot} is the sum of all the intracellular ionic currents of the single cell model, C_m is the membrane capacitance of the cell (57 pF), R_{gap} is the gap junction resistivity and V_{net} is the voltage difference between 4 neighbouring cells. A value of R_{gap} of 1 GΩ was adopted from the physiological range of coupling found in literature [6]. The model consisted of 50x50 central SAN cells, an estimate of the number of cells (∼5000) from which the stimulus is seen to originate [7]. Simulations lasted 20 s.

The Ca^{2+} permeabilities (P_{CaL}, P_{CaT}), the maximal conductances (g_{Kr}, g_{Ks}, g_{Kur}, g_{Na}, g_f, g_{to}), the maximal activity of the Na^+/K^+ pump and the Na^+/Ca^{2+} exchanger (I_{NaKmax}, K_{NaCa}) of the Fabbri model were randomized to take into account the biological variability by multiplying them by scaling coefficients extracted from a log-normal distribution. $\sigma = 0.1$, 0.2, 0.3 and 0.4 values of the standard deviation of the distribution were used.

2.2. Cell type density and distribution

Simulations with $R_{gap} = \infty$ (uncoupled cells) were run in order to investigate how many cells did not show spontaneous electrical activity following parameter randomization. The results are shown in table 1. For every σ, two additional levels of density D were tested:

- 40% : an approximation of the amount of fibrotic tissue found in adult human subjects under physiological conditions [1];
- 60% : reflecting a condition of upregulated fibrosis.

Being non-spontaneous cells in the uncoupled condition less than 40% and 60% for each σ (Table 1), the same cell parameters were used to reach a total amount of 1000 and 1500 cells, respectively. To evaluate the effects of diffuse vs. patchy fibrosis, random and cluster distribution of cells inside the tissue were tested. The latter was considered only in the D = 40% and 60% cases, so that to obtain randomly-distributed, non-overlapping clusters of 10x10 cells. The same cell positions were used across different simulations to exclude the effects of different distributions. The same workflow was adopted to simulate the effect of scar tissue - modeled as cells that did not show any connection with neighbours ($R_{gap} = \infty$) - and of fibroblasts, for which the active model of atrial fibroblast by Morgan et al. [8] was used.

2.3. Features extraction

Cells were considered as beating if they had at least 3 action potentials (AP) during the last 5 s of simulation. CL was computed as the difference in time between two overshoots (OS > 0 mV) of the AP of every cell.

3. Results

As one would expect, the increase of σ leads to a growing number of non-spontaneous cells (in an uncoupled condition), as shown in Table 1.

Table 1. Results of the uncoupled cells simulation: the number of non-spontaneous cells grows with σ (standard deviation of the log-normal distribution).

σ	**0.1**	**0.2**	**0.3**	**0.4**
Non-spont. cells	1 (0%)	126 (5.0%)	357 (14.3%)	584 (23.4%)

Despite this, when the cells are coupled ($R_{gap} = 1$ GΩ), all of them show rhythmic electrical activity, even with D = 40% and 60%. The only exception is D = 60% and $\sigma = 0.1$, where 18 cells do not beat. From the bottom left panel (CL of non-spontaneous, D = 60%) of Figure 1, it can be seen that the CL of this condition, being 438 ms, is consistently shorter than the CL of the uncoupled condition (829 ms).

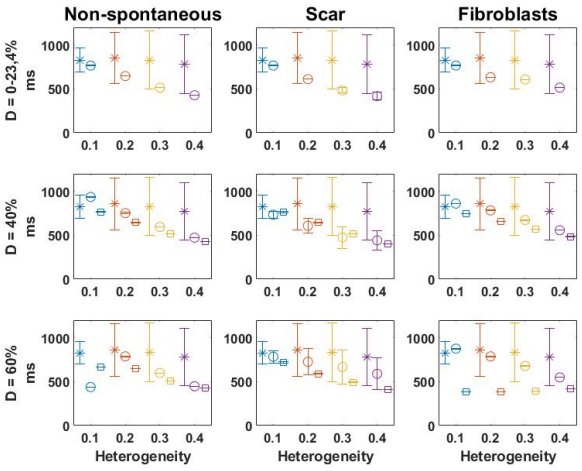

Figure 1. CLs of the tissue containing non-spontaneous cells, unexcitable cells and fibroblasts at different heterogeneities (σ) and densities (D). Asterisks ($*$) identify simulations with uncoupled cells, whereas circles ($\circ$) and squares ($\square$) identify simulations with random and cluster distribution, respectively. Mean values ± std.

This is probably due to the behaviour of these

irregularly-beating 18 cells. In fact, some of these cells actually show a rhythmic and stable depolarization, but without reaching the 0 mV threshold, whereas others show atypical electrical activity. Examples of these cells are shown in Figure 2.

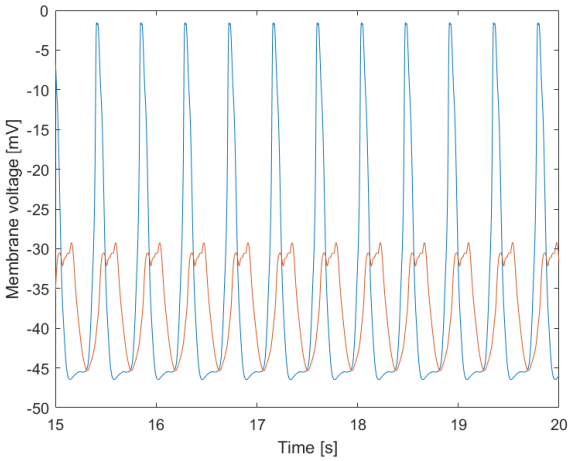

Figure 2. Examples of membrane voltage traces of two of the 18 irregularly-beating cells of condition D = 60%, $\sigma = 0.1$, in presence of non-spontaneous cells.

Particularly, the partition of these 18 cells into two groups elicits a spiral wave-like activity around the two clusters (Figure 3).

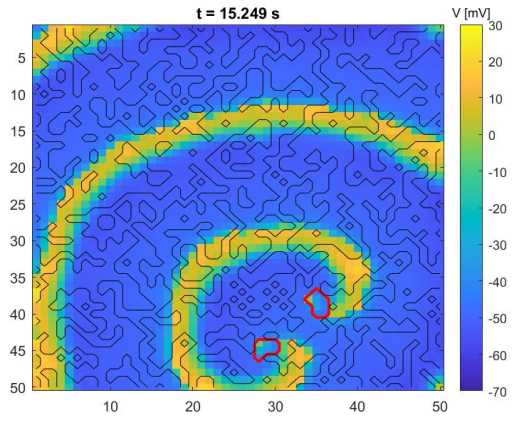

Figure 3. Color map showing the electrical activity of the 2D tissue with randomly-distributed non-spontaneous cells (in black): D = 60%, $\sigma = 0.1$. The spiral wave-like pattern is established around the two clusters of the 18 irregularly-beating cells (in red).

Despite this, the cells manage to synchronize their frequency as in all other coupled conditions, as shown by the negligible dispersion of the CL (Figure 1, first column). Plus, the average CL is reduced with an increase in cellular heterogeneity, being almost halved from $\sigma = 0.1$ to $\sigma = 0.4$ (e.g. D = 40% condition: from 936 ms to 473 ms). The density of non-spontaneous cells prolongs the average CL whereas the partitioning of non-spontaneous cells into clusters shortens it.

If scars are present, the results show that all non-scar cells are beating regardless of the heterogeneity of the tissue and the type of cell distribution (Figure 4). However, when unexcitable cells are randomly distributed, the tissue fails to fully synchronize its frequency: the CL sees a growing dispersion with an increase in D and σ (Figure 1, central column). As for the presence of non-spontaneous

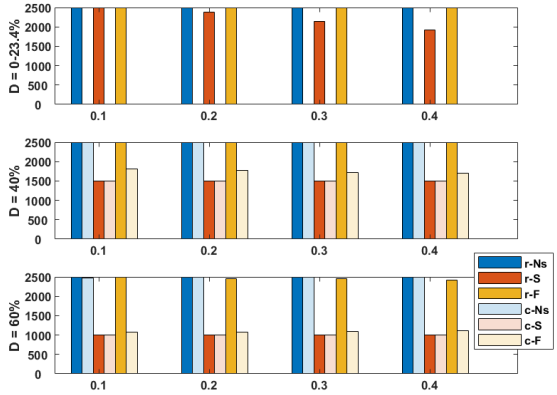

Figure 4. Number of beating cells inside the tissue at different heterogeneities (σ) and densities (D). r-: random distribution; c-: cluster distribution; Ns = non-spontaneous; S = scar; F = fibroblasts.

cells, average CL decreases with σ and cluster distribution. Similarly, D prolongs the CL (e.g. with $\sigma = 0.1$, from D = 0% to 60%, CL changes from 765 ms to 784 ms).

The presence of fibroblasts determines similar CL trends as in the previous conditions. Exceptions are represented by the D = 60%, $\sigma = 0.1 - 0.3$ cases, where the CL of the cluster distributions are consistently lower than that of the random ones. Regarding the number of beating cells, Figure 4 shows that - in the cluster condition - a large amount of cell is not showing rhythmic activity. This is because SAN myocytes do not manage to drive the inner fibroblasts forming the clusters, which are being shielded by the outer ones (of which however the most external ones are being driven by SAN cells).

4. Discussion and Conclusion

The results show the following evidences. First of all, increasing the density of the three cell phenotypes (non-spontaneous, scar and fibroblast) determines a

prolongation of the average CL. Considering that the maximal prolongation is 24% (fibroblasts presence, $\sigma = 0.2$) even when consistently different densities (5% vs 60%) are compared, it can be stated that the SAN is overall robust to a high presence of non-myocardial cells and manages to supply a physiologic and synchronized rate. Indeed, besides fibroblasts, non-spontaneous cells - also defined as "silent" or "dormant" - have been identified inside the SAN, and are believed to participate in the entrainment process [9]. Cell distribution has an even stronger effect on the CL. Grouping non-spontaneous cells in clusters determines a shortening of the CL, with respect to the random distribution condition. When scars are considered, cluster distributions leads to a lengthening of the average CL. These effects can be explained in terms of source-sink: with cluster distribution, spontaneous cells establish less connections with electrical loads (non-spontaneous cells) that would prolong their diastolic depolarization phase. With unexcitable cells instead, clusters determine a condition in which faster cells show more connections with neighbours. As a consequence, they are slowed down with respect to the random distribution condition, where they face more electrical barriers ($R_{gap} = \infty$) that protect them from being slowed. However, when D = 60%, some cluster can fall near the border of the matrix, shielding fast-pacing cells that are thus able to deliver higher rates.

An interesting role is played by the fibroblasts: being their resting potential more depolarized than the membrane potential of SAN cells during diastole, they act as current sources, speeding up the DD phase. However, they simultaneously reduce the OS. This reduced strength during the upstroke brings some SAN myocyte to not reaching the $0\,\mathrm{mV}$ threshold, besides preventing fibroblasts clusters to be driven by them. Thus, on one hand fibroblasts exert a protective role, increasing the robustness of diastolic depolarization; on the other one, they act as an electrical load during the upstroke, undermining SAN ability to self-depolarize and electrically drive them.

An additional evidence is that CL synchronization is reached in almost every condition, showing the robustness of the SAN in delivering a rhythmic and stable depolarization even when the beating myocytes are only a fraction of the tissue. Unfortunately, this is not true in the presence of randomly-distributed unexcitable cells, meaning that the condition mimicking a scar represents an unrealistic or pathological condition constituting a substrate for arrhythmias. Another critical condition is represented by low levels of cellular heterogeneity. In the D = 60% and $\sigma = 0.1$ case of non-spontaneous cells presence (Figures 1-3), healthy myocytes are too weak to drive all the tissue. This fact causes the establishment of two groups of rhythmically but irregularly-beating cells that act as functional blocks. Consequently, a re-entry-like mechanism is elicited, bringing to a tachycardic condition (CL = 438 ms, 137 bpm). Similar re-entrant waves appear around clusters of fibroblasts when D = 60%, thus determining high rates.

The purpose of this work was to elucidate the effects of conditions related to fibrosis inside the sinoatrial node. In summary, the amount of non-spontaneous myocytes influences the basal CL; unexcitable myocytes represent a pathological condition, mimicking the presence of scars; finally, fibroblasts exert a dual role - both protective and detrimental - on SAN tissue, especially when clustered. Limitations of the present study include the simplification of the SAN structure and the absence of the electrotonic influence of the atrium.

References

[1] Csepe TA, et al. Novel application of 3d contrast-enhanced cmr to define fibrotic structure of the human sinoatrial node in vivo. Eur Heart J Cardiovasc Imaging 2017; 18(1):862–869.

[2] Csepe TA, et al. Human sinoatrial node structure: 3d microanatomy of sinoatrial conduction pathways. Prog Biophys Mol Biol 2016;120(1):164–178.

[3] Pellman J, et al. Myocyte-fibroblast communication in cardiac fibrosis and arrhythmias: Mechanisms and model systems. J Mol Cell Cardiol 2016;94:22–31.

[4] Oren RV, Clancy CE. Determinants of heterogeneity, excitation and conduction in the sinoatrial node: A model study. PLOS Comput Biol 12 2010;6:1–13.

[5] Fabbri A, et al. Computational analysis of the human sinus node action potential: model development and effects of mutations. J Physiol Lond 2017;95(7):2365–2396.

[6] Inada S, et al. Importance of gradients in membrane properties and electrical coupling in sinoatrial node pacing. PLOS ONE 2014;9(4):e94565.

[7] Bleeker WK, et al. Functional and morphological organization of the rabbit sinus node. Circ Res 1980; 46(1):11–22.

[8] Morgan R, et al. Slow conduction in the border zones of patchy fibrosis stabilizes the drivers for atrial fibrillation: Insights from multi-scale human atrial modeling. Frontiers in Physiology 2016;7:474.

[9] Kim MS, et al. Heterogeneity of calcium clock functions in dormant, dysrhythmically and rhythmically firing single pacemaker cells isolated from SA node. Cell Calcium 2018; 74:168–179.

Address for correspondence:

Stefano Severi

Department of Electrical, Electronic and Information Engineering, University of Bologna,

Via dell'Università 50, 47522 Cesena (FC), Italy

stefano.severi@unibo.it